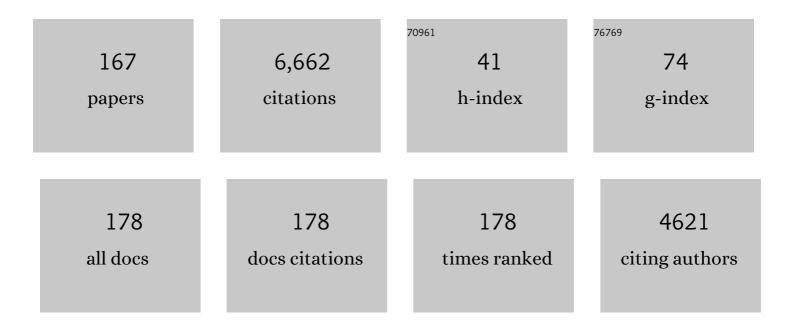
## Raman Singh

List of Publications by Year in descending order

Source: https://exaly.com/author-pdf/3907531/publications.pdf Version: 2024-02-01



#	Article	IF	CITATIONS
1	In vitro degradation and mechanical integrity of calcium-containing magnesium alloys in modified-simulated body fluid. Biomaterials, 2008, 29, 2306-2314.	5.7	491
2	Protecting copper from electrochemical degradation by graphene coating. Carbon, 2012, 50, 4040-4045.	5.4	409
3	Long-term durability of basalt- and glass-fibre reinforced polymer (BFRP/GFRP) bars in seawater and sea sand concrete environment. Construction and Building Materials, 2017, 139, 467-489.	3.2	359
4	Effect of sustained load and seawater and sea sand concrete environment on durability of basalt- and glass-fibre reinforced polymer (B/GFRP) bars. Corrosion Science, 2018, 138, 200-218.	3.0	205
5	Durability study on interlaminar shear behaviour of basalt-, glass- and carbon-fibre reinforced polymer (B/G/CFRP) bars in seawater sea sand concrete environment. Construction and Building Materials, 2017, 156, 985-1004.	3.2	192
6	Durability of fiber reinforced polymer (FRP) in simulated seawater sea sand concrete (SWSSC) environment. Corrosion Science, 2018, 141, 1-13.	3.0	171
7	Magnesium alloys as body implants: Fracture mechanism under dynamic and static loadings in a physiological environment. Acta Biomaterialia, 2012, 8, 916-923.	4.1	157
8	Magnesium Implants: Prospects and Challenges. Materials, 2019, 12, 136.	1.3	142
9	Corrosion fatigue fracture of magnesium alloys in bioimplant applications: A review. Engineering Fracture Mechanics, 2015, 137, 97-108.	2.0	127
10	Theoretical model for seawater and sea sand concrete-filled circular FRP tubular stub columns under axial compression. Engineering Structures, 2018, 160, 71-84.	2.6	119
11	Studies on blends of epoxy-functionalized hyperbranched polymer and epoxy resin. Journal of Materials Science, 2003, 38, 147-154.	1.7	118
12	A Review of Stress-Corrosion Cracking and Corrosion Fatigue of Magnesium Alloys for Biodegradable Implant Applications. Jom, 2015, 67, 1143-1153.	0.9	102
13	Thermal and mechanical properties of alkali-activated slag paste, mortar and concrete utilising seawater and sea sand. Construction and Building Materials, 2018, 159, 704-724.	3.2	101
14	Graphene: The Thinnest Known Coating for Corrosion Protection. Jom, 2014, 66, 637-642.	0.9	100
15	The role of microstructure in localized corrosion of magnesium alloys. Metallurgical and Materials Transactions A: Physical Metallurgy and Materials Science, 2004, 35, 2525-2531.	1.1	98
16	Evaluating the stress corrosion cracking susceptibility of Mg–Al–Zn alloy in modified-simulated body fluid for orthopaedic implant application. Scripta Materialia, 2008, 59, 175-178.	2.6	94
17	Electrochemical impedance spectroscopic investigation of the role of alkaline pre-treatment in corrosion resistance of a silane coating on magnesium alloy, ZE41. Electrochimica Acta, 2011, 56, 3790-3798.	2.6	94
18	In-vitro characterization of stress corrosion cracking of aluminium-free magnesium alloys for temporary bio-implant applications. Materials Science and Engineering C, 2014, 42, 629-636.	3.8	88

#	Article	IF	CITATIONS
19	Corrosion fatigue of a magnesium alloy in modified simulated body fluid. Engineering Fracture Mechanics, 2015, 137, 2-11.	2.0	87
20	Mechanical properties of seawater and sea sand concrete-filled FRP tubes in artificial seawater. Construction and Building Materials, 2018, 191, 977-993.	3.2	82
21	Durability of seawater and sea sand concrete filled filament wound FRP tubes under seawater environments. Composites Part B: Engineering, 2020, 202, 108409.	5.9	78
22	Development of Self-Healing Coatings Based on Linseed Oil as Autonomous Repairing Agent for Corrosion Resistance. Materials, 2014, 7, 7324-7338.	1.3	70
23	Electrochemical investigation of the influence of laser surface melting on the microstructure and corrosion behaviour of ZE41 magnesium alloy – An EIS based study. Corrosion Science, 2011, 53, 1505-1514.	3.0	69
24	Stress corrosion cracking of a recent rare-earth containing magnesium alloy, EV31A, and a common Al-containing alloy, AZ91E. Corrosion Science, 2013, 71, 1-9.	3.0	68
25	Stress corrosion cracking and corrosion fatigue characterisation of MgZn1Ca0.3 (ZX10) in a simulated physiological environment. Journal of the Mechanical Behavior of Biomedical Materials, 2017, 65, 634-643.	1.5	66
26	Mechanical integrity of magnesium alloys in a physiological environment: Slow strain rate testing based study. Engineering Fracture Mechanics, 2013, 103, 94-102.	2.0	65
27	Controlling hydrogen environment and cooling during CVD graphene growth on nickel for improved corrosion resistance. Carbon, 2018, 127, 131-140.	5.4	64
28	Bond-slip behaviour between FRP tubes and seawater sea sand concrete. Engineering Structures, 2019, 197, 109421.	2.6	63
29	Hydrogen-induced-cracking in magnesium alloy under cathodic polarization. Scripta Materialia, 2007, 57, 579-581.	2.6	62
30	Influence of bovine serum albumin in Hanks' solution on the corrosion and stress corrosion cracking of a magnesium alloy. Materials Science and Engineering C, 2017, 80, 335-345.	3.8	62
31	In vitro investigation of biodegradable polymeric coating for corrosion resistance of Mg-6Zn-Ca alloy in simulated body fluid. Materials Science and Engineering C, 2014, 42, 91-101.	3.8	60
32	Representing crack growth in additively manufactured Ti-6Al-4V. International Journal of Fatigue, 2018, 116, 610-622.	2.8	59
33	Durability of pultruded GFRP tubes subjected to seawater sea sand concrete and seawater environments. Construction and Building Materials, 2020, 245, 118399.	3.2	57
34	Role of Nanostructure in Electrochemical Corrosion and High Temperature Oxidation: A Review. Metallurgical and Materials Transactions A: Physical Metallurgy and Materials Science, 2014, 45, 5799-5822.	1.1	56
35	Axial compression tests on seawater and sea sand concrete-filled double-skin stainless steel circular tubes. Engineering Structures, 2018, 176, 426-438.	2.6	56
36	Oxidation resistance of nanocrystalline vis-Ã-vis microcrystalline Fe–Cr alloys. Corrosion Science, 2009, 51, 316-321.	3.0	54

#	Article	IF	CITATIONS
37	Additively manufactured Ti-6Al-4V replacement parts for military aircraft. International Journal of Fatigue, 2019, 124, 227-235.	2.8	51
38	Effects of UV radiation, moisture and elevated temperature on mechanical properties of GFRP pultruded profiles. Construction and Building Materials, 2020, 231, 117137.	3.2	51
39	Corrosion of Mg alloy AZ91 – the role of microstructure. Corrosion Engineering Science and Technology, 2004, 39, 346-350.	0.7	48
40	Electrochemical characteristics of nano and microcrystalline Fe–Cr alloys. Journal of Materials Science, 2012, 47, 6118-6124.	1.7	47
41	Degradation of graphene coated copper in simulated proton exchange membrane fuel cell environment: Electrochemical impedance spectroscopy study. Journal of Power Sources, 2017, 362, 366-372.	4.0	47
42	Crack Growth in a Range of Additively Manufactured Aerospace Structural Materials. Aerospace, 2018, 5, 118.	1.1	43
43	An all-gluten biocomposite: Comparisons with carbon black and pine char composites. Composites Part A: Applied Science and Manufacturing, 2019, 120, 42-48.	3.8	42
44	Mechanical properties of pultruded GFRP profiles under seawater sea sand concrete environment coupled with UV radiation and moisture. Construction and Building Materials, 2020, 258, 120369.	3.2	42
45	Effect of Fibers Configuration and Thickness on Tensile Behavior of GFRP Laminates Exposed to Harsh Environment. Polymers, 2019, 11, 1401.	2.0	41
46	Bond performance between FRP tubes and seawater sea sand concrete after exposure to seawater condition. Construction and Building Materials, 2020, 265, 120342.	3.2	41
47	Influence of circumferential notch and fatigue crack on the mechanical integrity of biodegradable magnesiumâ€based alloy in simulated body fluid. Journal of Biomedical Materials Research - Part B Applied Biomaterials, 2011, 96B, 303-309.	1.6	40
48	Crack growth: Does microstructure play a role?. Engineering Fracture Mechanics, 2018, 187, 190-210.	2.0	40
49	Grain growth behaviour and consolidation of ball-milled nanocrystalline Fe–10Cr alloy. Materials Science & Engineering A: Structural Materials: Properties, Microstructure and Processing, 2008, 494, 253-256.	2.6	39
50	Durable Corrosion Resistance of Copper Due to Multi-Layer Graphene. Materials, 2017, 10, 1112.	1.3	39
51	Role of nitrite addition in chloride stress corrosion cracking of a super duplex stainless steel. Corrosion Science, 2010, 52, 113-117.	3.0	38
52	Graphene coating on a nickel-copper alloy (Monel 400) for microbial corrosion resistance: Electrochemical and surface characterizations. Corrosion Science, 2021, 182, 109299.	3.0	37
53	Nano-structured palladium impregnate graphitic carbon nitride composite for efficient hydrogen gasÂsensing. International Journal of Hydrogen Energy, 2020, 45, 10623-10636.	3.8	36
54	Stress corrosion cracking of an extruded magnesium alloy (ZK21) in a simulated body fluid. Engineering Fracture Mechanics, 2018, 201, 47-55.	2.0	35

#	Article	IF	CITATIONS
55	Biological Self-Healing of Cement Paste and Mortar by Non-Ureolytic Bacteria Encapsulated in Alginate Hydrogel Capsules. Materials, 2020, 13, 3711.	1.3	35
56	Durability of glass-fibre-reinforced polymer composites under seawater and sea-sand concrete coupled with harsh outdoor environments. Advances in Structural Engineering, 2021, 24, 1090-1109.	1.2	35
57	Validity of a new fracture mechanics technique for the determination of the threshold stress intensity factor for stress corrosion cracking (KIscc) and crack growth rate of engineering materials. Engineering Fracture Mechanics, 2008, 75, 1623-1634.	2.0	33
58	Influence of Cold Spray Parameters on Bonding Mechanisms: A Review. Metals, 2021, 11, 2016.	1.0	31
59	Corrosion of 2205 Duplex Stainless Steel Weldment in Chloride Medium Containing Sulfate-Reducing Bacteria. Metallurgical and Materials Transactions A: Physical Metallurgy and Materials Science, 2008, 39, 2689-2697.	1.1	30
60	Fabrication and oxidation resistance of nanocrystalline Fe10Cr alloy. Journal of Materials Science, 2010, 45, 4884-4888.	1.7	30
61	Investigations into stress corrosion cracking behaviour of AZ91D magnesium alloy in physiological environment. Procedia Engineering, 2011, 10, 518-523.	1.2	30
62	Influence of Zeolite Coating on the Corrosion Resistance of AZ91D Magnesium Alloy. Materials, 2014, 7, 6092-6104.	1.3	30
63	In-vitro biodegradation and corrosion-assisted cracking of a coated magnesium alloy in modified-simulated body fluid. Materials Science and Engineering C, 2017, 78, 278-287.	3.8	30
64	Plastics—Villain or Hero? Polymers and Recycled Polymers in Mineral and Metallurgical Processing—A Review. Materials, 2019, 12, 655.	1.3	30
65	Laser assisted modification of surface microstructure for localised corrosion resistance of magnesium alloys. Surface Engineering, 2007, 23, 107-111.	1.1	29
66	Modelling of mode-I stable crack growth under hydrogen assisted stress corrosion cracking. Engineering Fracture Mechanics, 2011, 78, 3153-3165.	2.0	29
67	Bimodal grain size distribution: an effective approach for improving the mechanical and corrosion properties of Fe–Cr–Ni alloys. Journal of Materials Science, 2012, 47, 7735-7743.	1.7	29
68	Circumferential notched tensile (CNT) testing of cast iron for determination of threshold (KISCC) for caustic crack propagation. Materials Science & Engineering A: Structural Materials: Properties, Microstructure and Processing, 2005, 407, 207-212.	2.6	28
69	Resistance of nanocrystalline vis-Ã-vis microcrystalline Fe–Cr alloys to environmental degradation and challenges to their synthesis. Philosophical Magazine, 2010, 90, 3233-3260.	0.7	28
70	Study of hydrogen concentration dependent growth of external annular crack in round tensile specimen using cohesive zone model. Engineering Fracture Mechanics, 2013, 106, 49-66.	2.0	28
71	Multi-layer graphene coating for corrosion resistance of Monel 400 alloy in chloride environment. Surface and Coatings Technology, 2019, 370, 227-234.	2.2	28
72	Determination of crack growth rate and threshold for caustic cracking (Klscc) of a cast iron using small circumferential notched tensile (CNT) specimens. Materials Science & Engineering A: Structural Materials: Properties, Microstructure and Processing, 2006, 425, 272-277.	2.6	27

Raman Singh

#	Article	lF	CITATIONS
73	A novel approach to the determination of the threshold for stress corrosion cracking (K ISCC) using round tensile specimens. Metallurgical and Materials Transactions A: Physical Metallurgy and Materials Science, 2006, 37, 2963-2973.	1.1	27
74	Stress corrosion cracking behavior of magnesium alloys EV31A and AZ91E. Materials Science & Engineering A: Structural Materials: Properties, Microstructure and Processing, 2013, 583, 169-176.	2.6	27
75	Corrosion fatigue of a magnesium alloy under appropriate human physiological conditions for bio-implant applications. Engineering Fracture Mechanics, 2017, 186, 134-142.	2.0	27
76	Behaviour of seawater and sea sand concrete filled FRP square hollow sections. Thin-Walled Structures, 2020, 148, 106596.	2.7	27
77	Resistance of Magnesium Alloys to Corrosion Fatigue for Biodegradable Implant Applications: Current Status and Challenges. Materials, 2017, 10, 1316.	1.3	26
78	A long aliphatic chain functional silane for corrosion and microbial corrosion resistance of steel. Progress in Organic Coatings, 2019, 127, 27-36.	1.9	26
79	Review of Requirements for the Durability and Damage Tolerance Certification of Additively Manufactured Aircraft Structural Parts and AM Repairs. Materials, 2020, 13, 1341.	1.3	26
80	Evaluation of caustic embrittlement susceptibility of steels by slow strain rate testing. Metallurgical and Materials Transactions A: Physical Metallurgy and Materials Science, 2005, 36, 1817-1823.	1.1	25
81	Investigation of hydrogen assisted cracking of a high strength steel using circumferentially notched tensile test. Materials Science & Engineering A: Structural Materials: Properties, Microstructure and Processing, 2012, 547, 86-92.	2.6	24
82	Load-strain model for concrete-filled double-skin circular FRP tubes under axial compression. Engineering Structures, 2019, 181, 629-642.	2.6	24
83	Corrosion behavior of twinningâ€induced plasticity (TWIP) steel. Materials and Corrosion - Werkstoffe Und Korrosion, 2013, 64, 231-235.	0.8	23
84	Corrosion of bare and silane-coated mild steel in chloride medium with and without sulphate reducing bacteria. Progress in Organic Coatings, 2017, 111, 231-239.	1.9	23
85	Understanding Fibre-Matrix Degradation of FRP Composites for Advanced Civil Engineering Applications: An Overview. Corrosion and Materials Degradation, 2018, 1, 27-41.	1.0	22
86	Theoretical model for concrete-filled stainless steel circular stub columns under axial compression. Journal of Constructional Steel Research, 2019, 157, 426-439.	1.7	22
87	Oxide Scale Morphology and Chromium Evaporation Characteristics of Alloys for Balance of Plant Applications in Solid Oxide Fuel Cells. Metallurgical and Materials Transactions A: Physical Metallurgy and Materials Science, 2013, 44, 193-206.	1.1	21
88	Long-Term Corrosion Protection of a Cupro-Nickel Alloy Due to Graphene Coating. Coatings, 2017, 7, 210.	1.2	21
89	Hydrogen gas sensing of nano-confined Pt/g-C3N4 composite at room temperature. International Journal of Hydrogen Energy, 2021, 46, 23962-23973.	3.8	21
90	Validation of a novel approach to determination of threshold for stress corrosion cracking (KISCC). Materials Science & Engineering A: Structural Materials: Properties, Microstructure and Processing, 2007, 452-453, 652-656.	2.6	20

#	Article	IF	CITATIONS
91	On the Growth of Fatigue Cracks from Material and Manufacturing Discontinuities Under Variable Amplitude Loading. Jom, 2015, 67, 1385-1391.	0.9	20
92	Multifunctional, Sustainable, and Biological Non-Ureolytic Self-Healing Systems for Cement-Based Materials. Engineering, 2022, 13, 217-237.	3.2	20
93	Synthesis, characterization and mechanical behaviour of an in situ consolidated nanocrystalline FeCrNi alloy. Journal of Materials Science, 2012, 47, 1562-1566.	1.7	19
94	Hexagonal Boron Nitride Impregnated Silane Composite Coating for Corrosion Resistance of Magnesium Alloys for Temporary Bioimplant Applications. Metals, 2017, 7, 518.	1.0	19
95	Role of caustic concentration and electrochemical potentials in caustic cracking of steels. Materials Science & Engineering A: Structural Materials: Properties, Microstructure and Processing, 2006, 441, 342-348.	2.6	18
96	Stress Corrosion Cracking of an Austenitic Stainless Steel in Nitrite-Containing Chloride Solutions. Materials, 2014, 7, 7799-7808.	1.3	18
97	Interplay of microbiological corrosion and alloy microstructure in stress corrosion cracking of weldments of advanced stainless steels. Sadhana - Academy Proceedings in Engineering Sciences, 2003, 28, 467-473.	0.8	17
98	Determination of threshold stress intensity factor for stress corrosion cracking (KISCC) of steel heat affected zone. Corrosion Science, 2009, 51, 2443-2449.	3.0	17
99	Stress corrosion cracking of a wrought Mg–Mn alloy under plane strain and plane stress conditions. Engineering Fracture Mechanics, 2013, 102, 180-193.	2.0	17
100	Appropriate Mechanochemical Conditions for Corrosion-Fatigue Testing of Magnesium Alloys for Temporary Bioimplant Applications. Jom, 2015, 67, 1137-1142.	0.9	16
101	Investigation of role of alloy microstructure in hydrogen-assisted fracture of AISI 4340 steel using circumferentially notched cylindrical specimens. Materials Science & Engineering A: Structural Materials: Properties, Microstructure and Processing, 2017, 698, 191-197.	2.6	16
102	Effects of CNT modified adhesives and silane chemical pre-treatment on CFRP/steel bond behaviour and durability. Construction and Building Materials, 2021, 273, 121803.	3.2	16
103	A Two-Step Silane Coating Incorporated with Quaternary Ammonium Silane for Mitigation of Microbial Corrosion of Mild Steel. ACS Omega, 2021, 6, 16913-16923.	1.6	16
104	Cracking of magnesium-based biodegradable implant alloys under the combined action of stress and corrosive body fluid: a review. Emerging Materials Research, 2013, 2, 219-228.	0.4	15
105	In Vitro Evaluation of Degradation of a Calcium Phosphate Coating on a Mg-Zn-Ca Alloy in a Physiological Environment. Corrosion, 2012, 68, 499-506.	0.5	14
106	Durable degradation resistance of graphene coated nickel and Monel-400 as bi-polar plates for proton exchange membrane fuel cell. Carbon, 2019, 151, 68-75.	5.4	14
107	Role of imposed potentials in threshold for caustic cracking susceptibility (KISCC): Investigations using circumferential notch tensile (CNT) testing. Corrosion Science, 2007, 49, 4386-4395.	3.0	13
108	Influence of Laser Processing Parameters on Microstructure and Corrosion Kinetics of Laser-Treated ZE41 Magnesium Alloy. Metallurgical and Materials Transactions A: Physical Metallurgy and Materials Science, 2013, 44, 2346-2357.	1.1	13

#	Article	IF	CITATIONS
109	Durability of seawater and sea sand concrete and seawater and sea sand concrete–filled fibre-reinforced polymer/stainless steel tubular stub columns. Advances in Structural Engineering, 2021, 24, 1074-1089.	1.2	13
110	Determination of threshold stress intensity for chloride stress corrosion cracking of solution-annealed and sensitized austenitic stainless steel by circumferential notch tensile technique. Corrosion Science, 2010, 52, 1985-1991.	3.0	12
111	Effect of chromium and aluminum addition on anisotropic and microstructural characteristics of ball milled nanocrystalline iron. Journal of Alloys and Compounds, 2016, 671, 164-169.	2.8	12
112	Near-Field Mapping of Localized Plasmon Resonances in Metal-Free, Nanomembrane Graphene for Mid-Infrared Sensing Applications. ACS Applied Nano Materials, 2018, 1, 6454-6462.	2.4	12
113	Bonded CFRP/Steel Systems, Remedies of Bond Degradation and Behaviour of CFRP Repaired Steel: An Overview. Polymers, 2021, 13, 1533.	2.0	12
114	Quantifying Corrosion between Carbon Fibre Reinforced Polymers (CFRP) and Steel Caused by High Temperature Marine Environments. Advances in Structural Engineering, 2014, 17, 1761-1770.	1.2	11
115	Relevance of high-temperature oxidation in life assessment and microstructural degradation of Cr-Mo steel weldments. Metallurgical and Materials Transactions A: Physical Metallurgy and Materials Science, 2000, 31, 3101-3108.	1.1	10
116	Threshold stress intensity factor and crack growth rate for stress corrosion cracking of simulated heat affected zone in caustic solution. Engineering Fracture Mechanics, 2011, 78, 13-26.	2.0	10
117	Structural Evolution during Milling, Annealing, and Rapid Consolidation of Nanocrystalline Fe–10Cr–3Al Powder. Materials, 2017, 10, 272.	1.3	10
118	Computing the Growth of Small Cracks in the Assist Round Robin Helicopter Challenge. Metals, 2020, 10, 944.	1.0	10
119	Efficient approach for cohesive zone based three-dimensional analysis of hydrogen-assisted cracking of a circumferentially notched round tensile specimen. International Journal of Hydrogen Energy, 2017, 42, 15943-15955.	3.8	9
120	Computing the Fatigue Life of Cold Spray Repairs to Simulated Corrosion Damage. Materials, 2021, 14, 4451.	1.3	9
121	Thermomechanical Manipulation of Crack-Tip Stress Field for Resistance to Stress Corrosion Crack Propagation. Metallurgical and Materials Transactions A: Physical Metallurgy and Materials Science, 2008, 39, 3217-3223.	1.1	8
122	Twinning-assisted environmental cracking: A new fracture mechanism for the crash-resistant twinning-induced plasticity steels. Scripta Materialia, 2012, 67, 943-946.	2.6	8
123	Electrochemical Investigations of Steels in Seawater Sea Sand Concrete Environments. Materials, 2021, 14, 5713.	1.3	8
124	Role of gaseous environment and secondary precipitation in microstructural degradation of Cr-Mo steel weldments at high temperatures. Metallurgical and Materials Transactions A: Physical Metallurgy and Materials Science, 1999, 30, 2103-2113.	1.1	6
125	Role of Imposed Potential in Expanding the Regime of Strain Rates for Caustic Cracking. Journal of the Electrochemical Society, 2007, 154, C451.	1.3	6
126	Studying the effect of sensitization on the threshold stress intensity and crack growth for chloride stress corrosion cracking of austenitic stainless steel using circumferential notch tensile technique. Engineering Fracture Mechanics, 2012, 82, 158-171.	2.0	6

#	Article	IF	CITATIONS
127	High Temperature Corrosion and Oxidation of Metals. Metals, 2019, 9, 942.	1.0	6
128	Thoughts on two approaches for accounting for the scatter in fatigue delamination growth curves. Composite Structures, 2021, 258, 113175.	3.1	6
129	Mechanical Alloying of Elemental Powders into Nanocrystalline (NC) Fe-Cr Alloys: Remarkable Oxidation Resistance of NC Alloys. Metals, 2021, 11, 695.	1.0	6
130	Electrochemical Corrosion Resistance of Mg Alloy ZK60 in Different Planes with Respect to Extrusion Direction. Metals, 2022, 12, 782.	1.0	6
131	Caustic stress corrosion cracking of a graphite cast iron component. Engineering Failure Analysis, 2004, 11, 199-206.	1.8	5
132	High Temperature Oxidation of Cr-Mo Steels in the Context of Accelerated Rupture Testing for Creep Life Prediction. Journal of Pressure Vessel Technology, Transactions of the ASME, 2007, 129, 454-459.	0.4	5
133	High-Temperature Oxidation of Cr-Mo Steels and Its Relevance to Accelerated Rupture Testing and Life Assessment of In-Service Components. Metallurgical and Materials Transactions A: Physical Metallurgy and Materials Science, 2007, 38, 1750-1759.	1.1	5
134	Circumferential Notched Tensile Testing for Correlation of the Stress Intensity Factor (K I ) and Stress Corrosion Crack Growth Rate. Metallurgical and Materials Transactions A: Physical Metallurgy and Materials Science, 2008, 39, 1475-1478.	1.1	5
135	Cohesive zone based axisymmetric modelling of hydrogen-assisted cracking in a circumferentially notched tensile specimen. International Journal of Hydrogen Energy, 2018, 43, 12530-12542.	3.8	5
136	Corrosion: Critical Challenge in Wider Use of Magnesium Alloys. Metals, 2018, 8, 127.	1.0	5
137	Austenitic Stainless-Steel Reinforcement for Seawater Sea Sand Concrete: Investigation of Stress Corrosion Cracking. Metals, 2021, 11, 500.	1.0	5
138	Nanocrystalline structure remarkably enhances oxidation resistance of Fe-20Cr-5Al alloy. Journal of Alloys and Compounds, 2022, 900, 163568.	2.8	5
139	Durability of Fibre Reinforced Polymers in Exposure to Dual Environment of Seawater Sea Sand Concrete and Seawater. Materials, 2022, 15, 4967.	1.3	5
140	Influence of Laser Surface Melting on the Microstructure and Corrosion Behaviour of ZE41 Magnesium Alloy. Materials Science Forum, 2009, 618-619, 263-268.	0.3	4
141	Circumventing Practical Difficulties in Determination of Threshold Stress Intensity for Stress Corrosion Cracking of Narrow Regions of Welded Structures. Metallurgical and Materials Transactions A: Physical Metallurgy and Materials Science, 2012, 43, 3202-3214.	1.1	4
142	Experimental Studies into the Analysis Required for the Durability Assessment of 7075 and 6061 Cold Spray Repairs to Military Aircraft. Aerospace, 2020, 7, 119.	1.1	4
143	Role of Surface Preparation in Corrosion Resistance Due to Silane Coatings on a Magnesium Alloy. Molecules, 2021, 26, 6663.	1.7	4
144	Biofilm Development on Carbon Steel by Iron Reducing Bacterium Shewanella putrefaciens and Their Role in Corrosion. Metals, 2022, 12, 1005.	1.0	4

#	Article	IF	CITATIONS
145	Investigations Using Smooth and Notched Specimens into Validity of Caustic Cracking Susceptibility Diagram. Metallurgical and Materials Transactions A: Physical Metallurgy and Materials Science, 2010, 41, 2328-2336.	1.1	3
146	A Simple Approach to the Determination of Threshold Stress Intensity for Stress Corrosion Cracking (K ISCC) and Crack Growth of Sensitized Austenitic Stainless Steel. Metallurgical and Materials Transactions A: Physical Metallurgy and Materials Science, 2011, 42, 2643-2651.	1.1	3
147	Threshold Stress Intensity for Stress Corrosion Cracking (K <sub>ISCC</sub> ) of a Magnesium Alloy in Physiological Environment. Materials Science Forum, 2011, 690, 487-490.	0.3	3
148	Resistance of Nanostructured Fe-Cr Alloys to Oxidative Degradation: Role of Zr and Cr Contents. Metallurgical and Materials Transactions A: Physical Metallurgy and Materials Science, 2015, 46, 1814-1824.	1.1	3
149	Effect of Milling Time on Properties of Mechanochemically Synthesized Nano ZnO. , 2010, , .		2
150	Environment-Assisted Cracking of Twinning Induced Plasticity (TWIP) Steel: Role of pH and Twinning. Metallurgical and Materials Transactions A: Physical Metallurgy and Materials Science, 2014, 45, 1979-1995.	1.1	2
151	Effect of lanthanide activated nano‣iO <sub>2</sub> on the corrosion behavior of silaneâ€based hybrid coatings on low carbon steel. Materials and Corrosion - Werkstoffe Und Korrosion, 2015, 66, 1223-1231.	0.8	2
152	Mechanical integrity ofÂmagnesium alloys forÂbiomedical applications. , 2015, , 179-204.		2
153	Introduction to a New Journal: Corrosion and Materials Degradation. Corrosion and Materials Degradation, 2018, 1, 1-2.	1.0	2
154	Distinct Advantages of Circumferential Notch Tensile (CNT) Testing in the Determination of a Threshold for Stress Corrosion Cracking (KISCC). Materials, 2021, 14, 5620.	1.3	2
155	Thermal scaling behavior of weldments of 9Cr-1Mo steel and its relevance to the life assessment of fossil fuel power plant components. Metallurgical and Materials Transactions A: Physical Metallurgy and Materials Science, 2002, 33, 3296-3297.	1.1	1
156	Laser assisted surface modification of AZ91 alloy: Microstructural and electrochemical study. Transactions of the Indian Institute of Metals, 2008, 61, 121-124.	0.7	1
157	Revisiting Stress Corrosion Cracking of Steel in Caustic Solutions for Developing Cracking Susceptibility Diagrams for Improved Applicability. Metallurgical and Materials Transactions A: Physical Metallurgy and Materials Science, 2012, 43, 1944-1955.	1.1	1
158	Investigation of the mechanical properties of graphitic carbon nitride pellet and film by simulation and nanoindentation experiments. Bulletin of Materials Science, 2022, 45, .	0.8	1
159	Using Thermomechanical Conditioning Cycles to Improve Fracture Toughness of Low Carbon Steel. Metallurgical and Materials Transactions A: Physical Metallurgy and Materials Science, 2009, 40, 1118-1125.	1.1	0
160	Role of Nanotechnology in Combating High Temperature Corrosion. , 2016, , 219-243.		0
161	Hydroxide melt induced corrosion of Ni at elevated temperatures under steam electrolysis conditions. International Journal of Hydrogen Energy, 2021, 46, 28406-28417.	3.8	0
162	Understanding Corrosion-Assisted Cracking of Magnesium Alloys for Bioimplant Applications. , 2016, , 343-346.		0

#	Article	IF	CITATIONS
163	Appropriate Corrosion-Fatigue Testing of Magnesium Alloys for Temporary Bioimplant Applications. , 2016, , 353-356.		0
164	Graphene Coating and Nanocrystalline Alloy Structure: Two Novel Nanotechnology Approaches for Remarkable Corrosion Resistance. , 0, 1, 1003.		0
165	Effect of Nanocrystalline Structure on the Oxidation Behavior of Fe–20Cr–3Al Alloy at High Temperatures. Oxidation of Metals, 2022, 97, 307.	1.0	0
166	Synthesis, Characterization, and Hydrogen Gas Sensing of ZnO/g-C3N4 Nanocomposite $\hat{a} \in$ . , 2021, 10, .		0
167	Recycling and Resource Recovery from Polymers. Polymers, 2022, 14, 2020.	2.0	0